Int J Adv Manuf Technol (2005) 25: 628–646
DOI 10.1007/s00170-004-2259-4

ORIGINAL ARTICLE

Yi Lu · Yoshimi Takeuchi · Ichiro Takahashi · Masahiro Anzai

An integrated system development for ball end mill design, creation and evaluation

Received: 11 February 2004 / Accepted: 18 May 2004 / Published online: 26 January 2005

Abstract The purpose of this paper is to provide a reasonable means to approach tool shape optimization of ball end mill for high-speed milling operation. The paper presents a new development of an integrated system for ball end mill design, creation and evaluation that is more flexible and more systematic than the commercially available tool fabrication systems.

The study consists of three major contents: (1) 3D-CAD/CAM system development for ball end mill design and creation, (2) fundamental investigations of cutting characteristics with different ball end mills, and (3) improvement of tool life and machining stabilization for high-speed milling by means of new tool shape proposals. These are explained in the following sections, respectively. Through the above developments and investigations, it is evidently found that the developed system shows great validity and possibility to realize tool shape optimization of the ball end mill.

Keywords Ball end mill · Cutting characteristics · High-speed milling · 3D-CAD/CAM system · Tool shape optimization

1 Introduction

In recent years, cutting operations have been taking on a bigger part in die and mold machining [1, 2], along with the rapid improvement of machine tools [3–6], cutting tools and high-speed milling technologies [7–10]. It appears that the demand to manufacture dies efficiently has increased. Ball end mills are regarded as the most suitable and widely used tools for use in die and mold cutting operations since they can be easily adapted to various workpieces that have complicated shapes, as well as be used for multiaxis control machining with collision-free tool path [11–13].

The development of cutting tools suitable for die machining is a major issue in the manufacturing field. From a viewpoint of tool manufacturing, cutting tool developments are strongly related to those of tool material, tool shape and coating treatment. Of major concern is how to find the most appropriate conditions among these three matters in order to achieve an optimal cutting operation.

Tool shape development depends on different tool types. This study deals with the ball nose part of a ball end mill, which has complex and problematic cutting edges. There are two essential requirements to efficiently conduct tool shape development:

1. Optimizaiton of tool fabrication process, and
2. Optimization of tool shape evaluation process in association with the tool fabrication process.

A flexible tool design and fabrication system is required with regard to item (1) above. A tool grinding CAM system supported by a 3D-CAD system can be one solution. With regard to item (2), it is necessary to establish the evaluation method with a feedback functional loop between the tool shape design and its investigation as soon as possible. Together with evaluations by conducting actual cutting experiments, geometric cutting simulations and analyses on the basis of a 3D-CAD system are also invaluable.

Based on the above two requirements, the capability of current commercially available tool grinding systems was investigated. 2D design systems of tools are broadly used in the industry today because of ease of application with all kinds of tool design and fabrication except for ball end mills. Since a ball end mill has intricate 3D helical cutting edge curve, rake face and flank face, it is hard to represent the entire shapes exactly by

Y. Lu (✉)
Department of Mechanical and Control Engineering,
The University of Electro-Communications,
1-5-1, Chofugaoka, Chofu-shi, Tokyo, 182-8585, Japan
E-mail: rlyi@ims.mce.uec.ac.jp
Tel.: +81-424-435411
Fax: +81-424-843327

Y. Takeuchi
Department of Computer-Controlled Mechanical Systems,
The Osaka University,
2-1, Yamadaoka, Suita-shi, Osaka, 565-0871, Japan

I. Takahashi · M. Anzai
Advanced Development and Supporting Center,
RIKEN (The Institute of Physical and Chemical Research),
2-1, Hirosawa, Wako-shi, Saitama, 351-0198, Japan

using a 2D design system only. In some cases, it is necessary for operators to manually correct various data when grinding a ball end mill. Accordingly, it may be said that currently available tool grinding systems are unable to handle well ball end mill shapes in terms of achieving tool shape optimization. Also, under these less than accurate grinding circumstances, one can understand the difficulty in manufacturing ball end mills, and that commercially available ball end mills hardly have any variance in their cutting edge shapes. While it seems that cutting experiments are the only means to rightly evaluate the tool cutting performance, the relationship between experimental results and tool shapes is not easily clarified. The left hand chart of Fig. 1 shows the flow of tool manufacturing with commercially available systems.

To break through the current less than ideal state of ball end mill fabrication, the study developed a ball end mill design and fabrication along with a corresponding evaluation system based on a 3D-CAD system. A ball end mill grinding CAM system used upon a 3D-CAD system can easily provide all the geometric information for ball end mill shapes and solve the omission problems encountered when using a 2D design system, i.e., the employment of a 3D-CAD system prevents the loss of tool shape information and enhances the variety of tool shape design and fabrication. Furthermore, the system allows us to evaluate the tool cutting performance by cutting experiments since the system can manufacture the same ball end mills as the geometrically defined ones. From a wider viewpoint, this system has a very real possibility of being readily applicable to evaluation systems containing cutting simulations, by using the same tool geometric models. More reasonable manufacturing development processes, like this, will lead to higher levels of tool shape development. The right hand chart of Fig. 1 shows an integrated system for ball end mill design, creation and evaluation explained in the study for tool shape optimization. Throughout this paper, the words "tool" and "ball end mill" are used with the same meaning.

2 Development of a ball end mill creation CAM system with 3D-CAD support

2.1 Outline of ball end mill design and fabrication 3D-CAD/CAM system

Figure 2 shows the flow of the ball end mill design and fabrication 3D-CAD/CAM system developed. In the study, a 3D-CAD modeller called DESIGNBASE (RICOH Co., Ltd.) and its kernel libraries are used to develop ball end mill grinding CAM software with C programming language. The CAM software consists of two processors: a main processor and a post processor. The main processor is developed to define the tool shapes of ball end mills, calculate the wheel posture for each defined tool shape, and generate the grinding location (GL) data of wheels in the 3D-CAD coordinate system. NC data can be obtained by post processing [14, 15], based on the information of wheel postures in GL data. Additionally, it is possible to arrange for a grinding operation check and a collision check, as well as a tool shape formation check on the 3D-CAD by displaying the GL data. These CAM functions and visualization activities provide higher flexibility and efficiency in regards to tool design and fabrication compared to commercially available tool grinding systems.

2.2 General information on tool shape design of the ball end mill

One cutting edge of the ball end mill is considered to consist of a ball end cutting edge and a peripheral cutting edge. The study focuses on the very intricate ball end cutting edge, having ambiguous definitions of shapes.

As shown in Fig. 3, a ball end cutting edge consists of a cutting edge curve, a rake face and a flank face. In addition, there are three parameters of a helix angle, a rake angle and a clearance angle that coincide with the above three edge shapes, respectively. As the cutting edge curve, i.e., the boundary curve

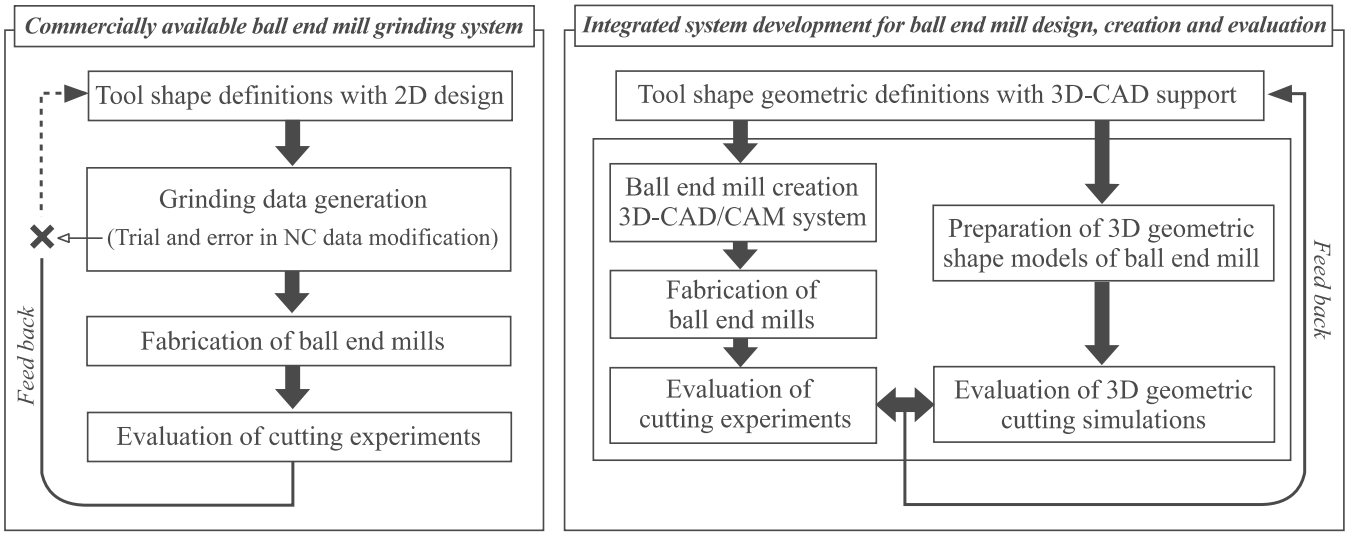

Fig. 1. Comparison between a commercially available ball end mill grinding system and an integrated system for ball end mill design, creation and evaluation

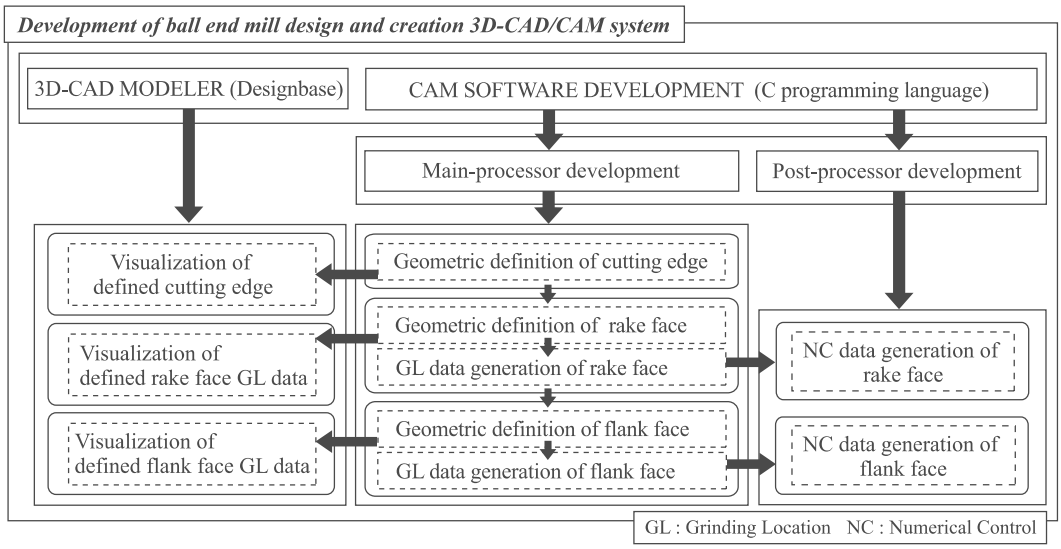

Fig. 2. Outline of a developed ball end mill design and fabrication 3D-CAD/CAM system

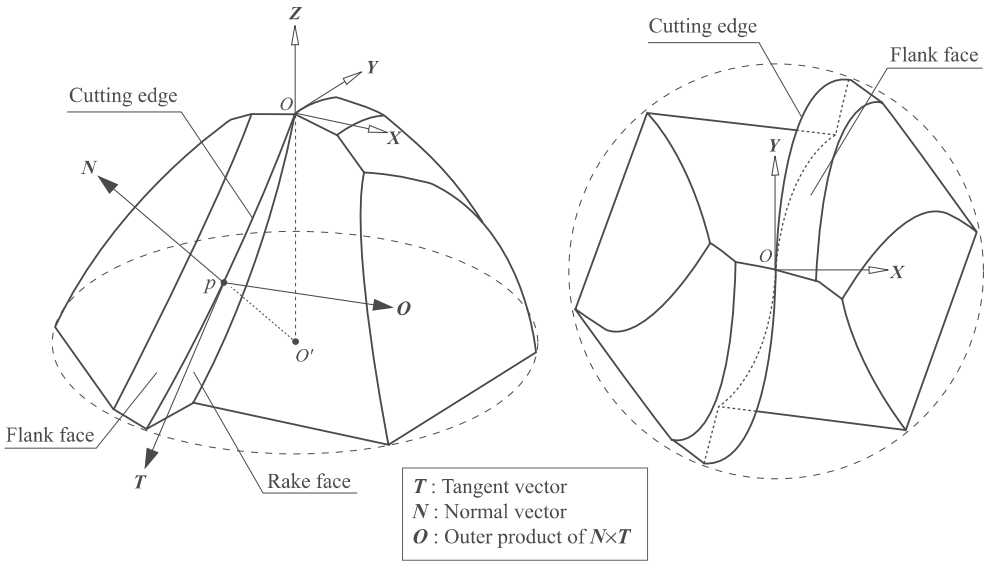

Fig. 3. General information about the tool shape design of a ball end mill

between the rake face and the flank face, varies together with the change in the helix angle, it makes tool design and fabrication difficult to handle. Along with it, the movement of grinding wheels is complex, and multiaxis control is required in some cases. Again, it seems that many difficulties must be overcome in designing perfect geometric tool shapes of ball end mills, and controlling the grinding wheel movements when the 2D tool design and fabrication systems are used.

In this study, a 3D-CAD system is adopted to provide the support for development of the CAM system. As shown in Fig. 3, a CAD coordinate system $O-XYZ$, matching tool axis OO' of the ball end mill with axis Z, is placed. In addition to the CAD coordinate system $O-XYZ$, a local coordinate system $p-NTO$ at optional point p on the cutting edge curve is available, too. In system $p-NTO$, normal vector **N** represents the direction pointing from tool center point O' to point p. Tangent vector **T** shows the tangential direction to the cutting edge curve at point p, and vector **O** is the outer product of $\mathbf{N}\times\mathbf{T}$. These three vectors are regarded as unit vectors throughout the paper.

2.3 Cutting edge curve creation

A helix angle is generally used as the parameter to describe the variation of a helical edge curve. A cutting edge curve model of a cylindrical end mill is shown on the left hand side of Fig. 4. Helical direction means the tangent direction to the cutting edge curve at optional point p_s. Angle λ_s between tangent vector **T** and tool axis vector $\mathbf{T}'$ is regarded as the helix angle at p_s. That is, in terms of optional point p_s, tangent vector $\mathbf{T}'$ to the straight cutting edge curve mn (helix angle = 0 degrees) and tangent vector **T** to the helical cutting edge curve ab create helix angle λ_s of a cylindrical end mill. In this case, normal vector **N** crosses both

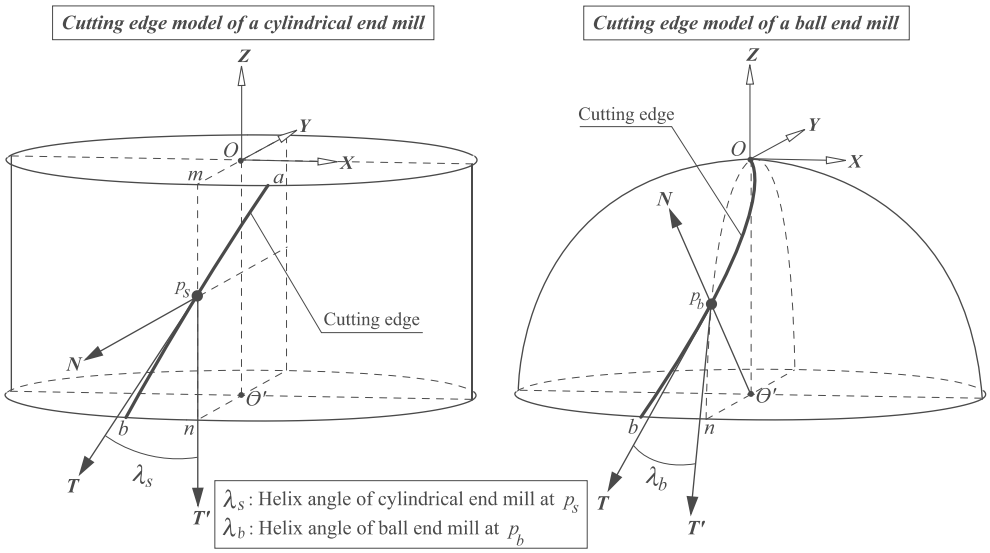

Fig. 4. Determination of helix angle λ_b to a ball end cutting edge curve

of the two tangent vectors **T** and **T**′ at a right angle. In general, the cutting edge curve of a cylindrical end mill can be designed and created using the constant value of a helix angle.

With the definition of a helix angle for a cylindrical end mill in mind, the determination of helix angle λ_b of a ball end mill is shown on the right hand side of Fig. 4. Helix angle λ_b of the ball end mill at optional point p_b refers to the angle consisting of tangent vector **T**′ to the straight cutting edge curve On (helix angle = 0 degrees) and tangent vector **T** to the helical cutting edge curve Ob. In this case, normal vector **N**, pointing from O' to p_b, crosses both of the two tangent vectors **T** and **T**′ at a right angle. The cutting edge curve function depends on the continuous changes in helix angle λ_b, which varies at different locations of the cutting edge. However, there are two boundary conditions that need to be satisfied for determining the cutting edge curve: (1) the helix angle starting at point O must be 0 degrees, and (2) the helix angle ending at point b must be the given value. The curved edge shape between the two locations is arbitrarily definable according to a designer's purpose.

Figure 5 displays an explanation of the ball end cutting edge curve function proposed in this study. A cylinder and a half sphere with the same radius represent a cylindrical end mill model and a ball end mill model, respectively. From the view of first section in Fig. 5, the helical edge curve ac, lying on the cylinder surface, is a straight line in substance. The angle $\angle cad$ corresponds to helix angle λ_s of the cylindrical end mill. It is assumed that a perpendicular line $p_s O_z$ comes from optional point p_s on the cylindrical end mill edge curve ac towards tool axis OO', intersecting with the surface of the ball end mill model at point p_b. Generalizing this concept, a new curve Oc can be generated by connecting all of the intersecting points lying on the half sphere surface. Helical curve Oc is defined in this study as the cutting edge curve of the ball end mill model.

As shown in the second and third section of Fig. 5, parameter ξ, the rotational angle in arc Od, is adopted to derive the function of the cutting edge curve Oc of the ball end mill. According to the geometric information from the cutting edge curve ac of the cylindrical end mill, the rotational angle φ in plane XY can be calculated and applied to determine the cutting edge location of the ball end mill. The cutting edge curve function of a ball end mill defined in the study is shown in Eq. 1 below:

$$p_b = \begin{pmatrix} X(\xi) \\ Y(\xi) \\ Z(\xi) \end{pmatrix} = \begin{pmatrix} -R\sin(k(1-\cos\xi))\sin\xi \\ -R\cos(k(1-\cos\xi))\sin\xi \\ -R(1-\cos\xi) \end{pmatrix}, \tag{1}$$

where $k = \tan\lambda_s$, $0 \le \xi \le \pi/2$.

Differentiating Eq. 1, the tangent vector to ball end cutting edge curve at optional point p_b is available. Additionally, helix angle λ_b at the point can be obtained as shown in Eq. 2:

$$\lambda_b = \begin{cases} \lambda_b = +|\cos^{-1}\left(\frac{1}{\sqrt{k^2\sin^4\xi+1}}\right)| & (0 \le \lambda_s < \pi) \\ \lambda_b = -|\cos^{-1}\left(\frac{1}{\sqrt{k^2\sin^4\xi+1}}\right)| & (-\pi/2 < \lambda_s < 0) \end{cases} \tag{2}$$

According to Eq. 2, Fig. 6 describes the variations of helix angle λ_b with different λ_s (30°, 10°, −10°, −30°). The figure indicates that the original definition of a ball end cutting edge satisfies the boundary conditions noted above.

For the sake of convenience, this paper uses the value of helix angle λ_b at the end point of cutting edge curve, which is equal to λ_s, to identify and name the ball end cutting edge curve. For example, a ball end mill with a helix angle of 30 degrees means that it has a helical cutting edge curve with a helix angle λ_b varing from 0 to 30 degrees. Based on the above definitions, Fig. 7 shows a defined ball end cutting edge curve with a helix angle of 30 degrees displayed on a 3D-CAD.

2.4 Rake face and flank face creation

This section deals with the rake face and flank face creation of a ball end mill determined by rake angle γ and clearance angle

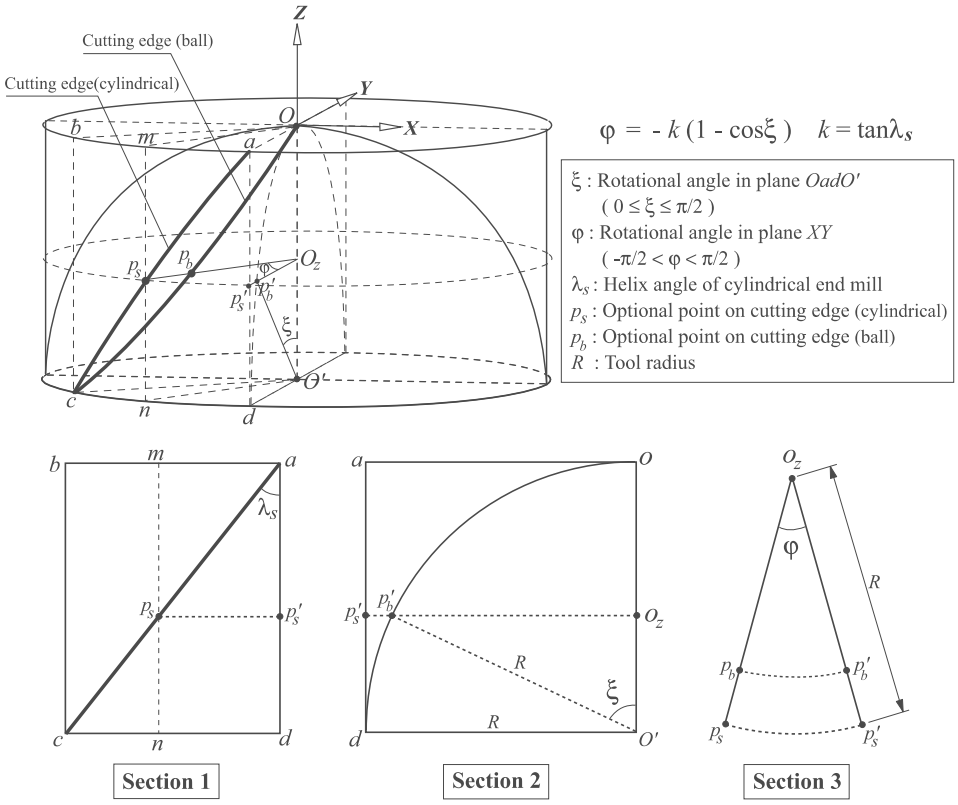

Fig. 5. Cutting edge curve determination of a ball end mill

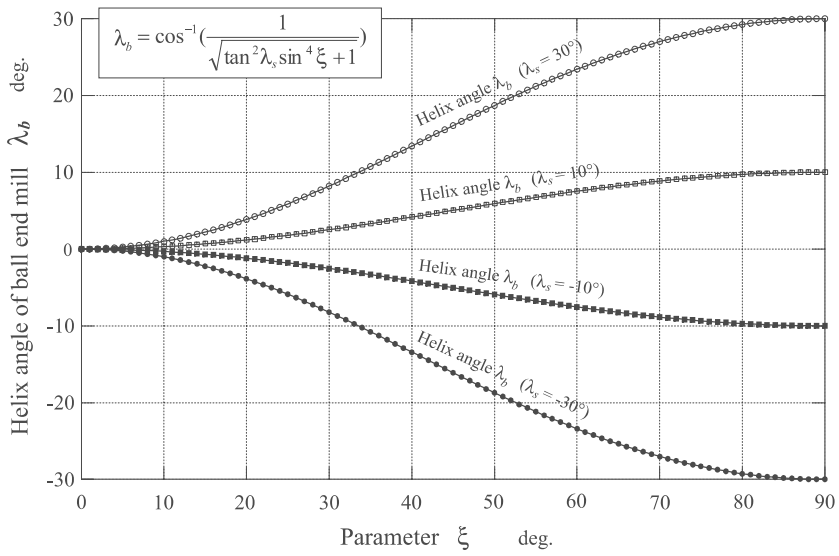

Fig. 6. Calculated helix angles λ_b of ball end mills

α as shown in Fig. 8a. In terms of optional point p on the cutting edge, normal vector **N**, tangent vector **T** and outer product **O** are available. An enlarged view of the cutting edge shape $ABCD$ and a local section $abcd$ consisting of vector **N** and **O**, are shown in Figs. 8b and 8c, respectively.

In Fig. 8c, it is very obvious that vector $\mathbf{N}_r$, showing the local rake face direction at point p, can be obtained by rotating vector $\mathbf{N}'$, the inverse normal vector **N**, in a clockwise direction by exact γ degrees around vector **T**. In the same way, vector $\mathbf{O}_f$, showing the local flank face direction, can be obtained by rotating vector $\mathbf{O}'$, inverse outer product **O**, in a counterclockwise direction by exact α degrees around vector **T**, too. The study defines angle γ for the rake angle and angle α for the clearance angle of the ball end mill at optional point p on the cutting edge curve. According to these definitions, it is possible to design and fabricate a ball end mill using constant rake angle and clearance angle values. In

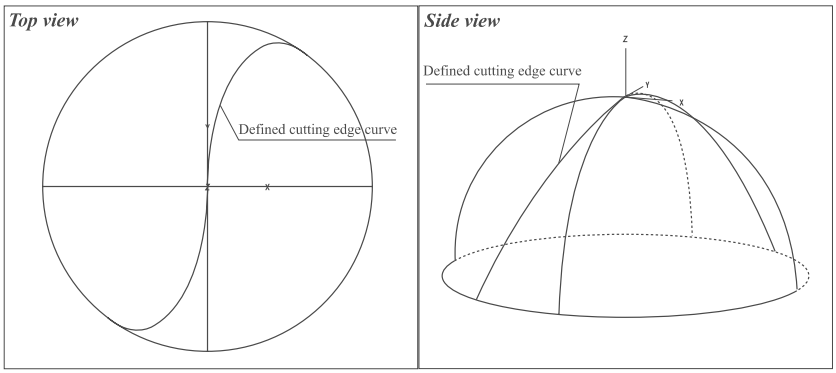

Fig. 7. Displayed cutting edge curve of a ball end mill on a 3D-CAD

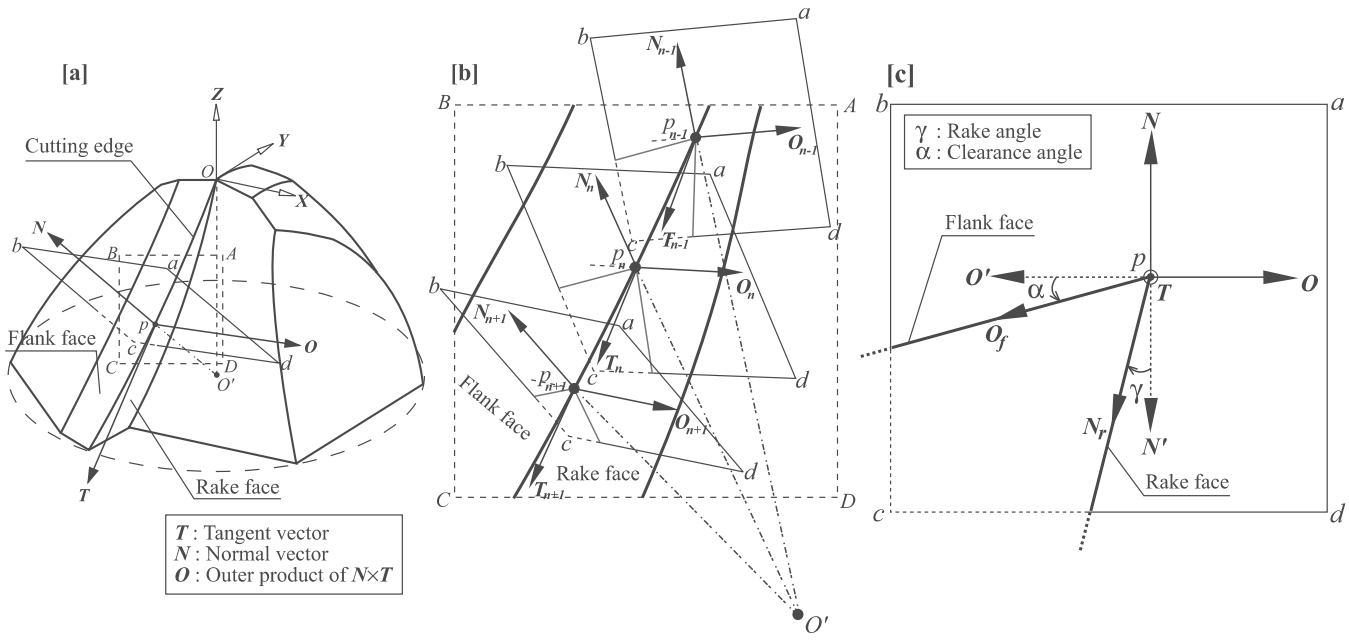

Fig. 8. Determinations of rake angle γ and clearance angle α of a ball end mill

practical steps, rake angle γ and clearance angle α are the given parameters set by the designers and then those are applied to the determination of spatial locations of the rake face and the flank face by the 3D-CAD/CAM system.

Figure 9 shows a defined rake face of a ball end mill displayed on a 3D-CAD. In addition to the tool shape visualization on a 3D-CAD, the developed CAM system calculates and outputs the wheel grinding location (GL) data for rake face fabri-

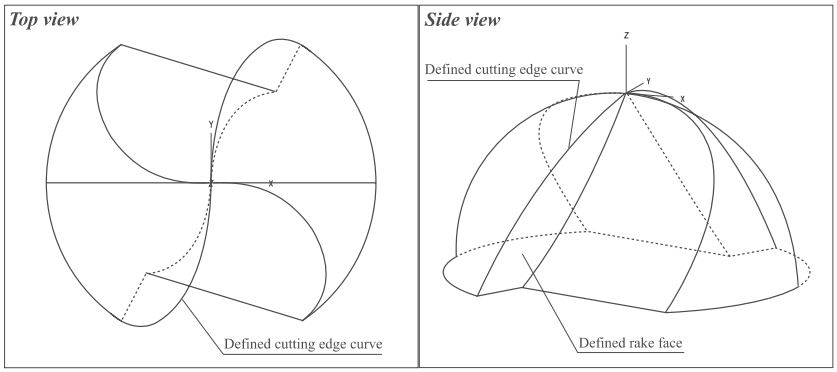

Fig. 9. Displayed rake face of a ball end mill on a 3D-CAD

cation. The left hand chart of Fig. 10 explains the GL data generation method by using the cutting edge definitions and wheel shape information such as wheel type, width and radius. The right hand chart of Fig. 10 shows an example of visualized rake face GL data with a straight wheel. It should be noted that these two pieces of information, wheel center point *C* and wheel axis vector **A**, together determine the wheel postures in 3D space. Through the same algorithm, flank face design and GL data generation are carried out by the definition of clearance angle. As a final creation, the part of a shoulder is designed and formed for a collision-free cutting operation. The completed images of a ball end mill are shown in Fig. 11.

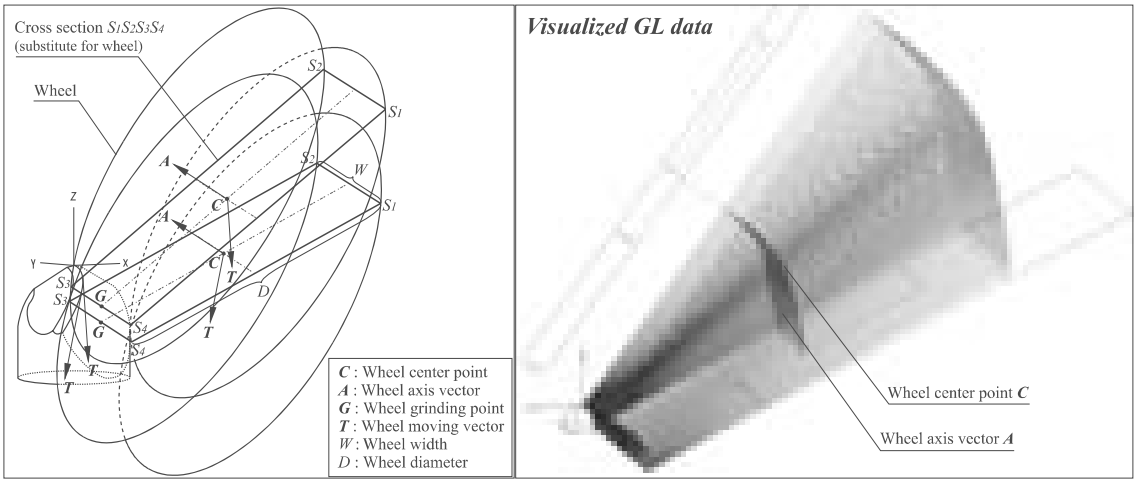

Fig. 10. Explanation of GL data generation with developed CAM system and visualization of generated rake face GL data on a 3D-CAD

Fig. 11. Displayed flank face and shoulder of a ball end mill on a 3D-CAD

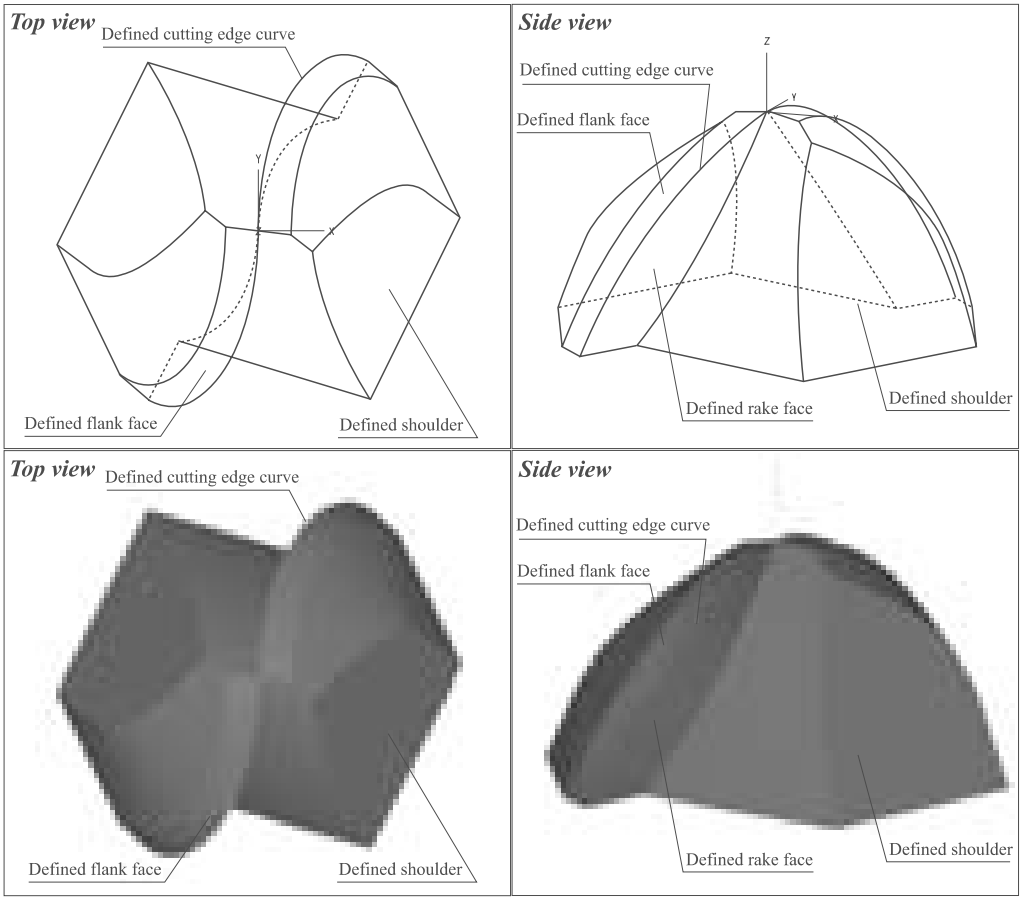

By means of the developed CAM system, tool shape definition, design and visualization are integrated on the 3D-CAD system. Furthermore, by representing the generated GL data, a collision check and data modification can be performed easily and efficiently before ball end mill fabrication.

The generated GL data by the main processor is converted into NC data by a post processor. The converted NC data is applied for ball end mill fabrication on a tool grinding machine.

2.5 Ball end mill trial grinding

A ball end mill trial grinding test was performed by the developed 3D-CAD/CAM system. A ball end mill, with helix angle $\lambda_b(30°)$, rake angle $\gamma(10°)$, clearance angle $\alpha(10°)$ with a diameter of 6 mm was designed and fabricated. Fine-grained cemented carbide was applied to the tool material and two types of wheels (straight and cup) were used for grinding. Figure 12 shows the structure of the tool grinding machine and conditions for ball end mill fabrication. The grinding test was conducted, and the designed ball end mill was successfully fabricated. The machining time was about 40 minutes. Figure 13 shows the designed ball end mill displayed on a 3D-CAD and the practically fabricated one. Without a doubt, the ball end mill was precisely fabricated as it was designed.

Figure 14 shows a result of tool radius accuracy measurement. The maximum error against the setting value was about 10 μm, i.e., the fabricated ball end mill is well within application range for a common machining.

According to the above investigations, it is evident that the ball end mill design and creation 3D-CAD/CAM system developed in the study is effectively applicable.

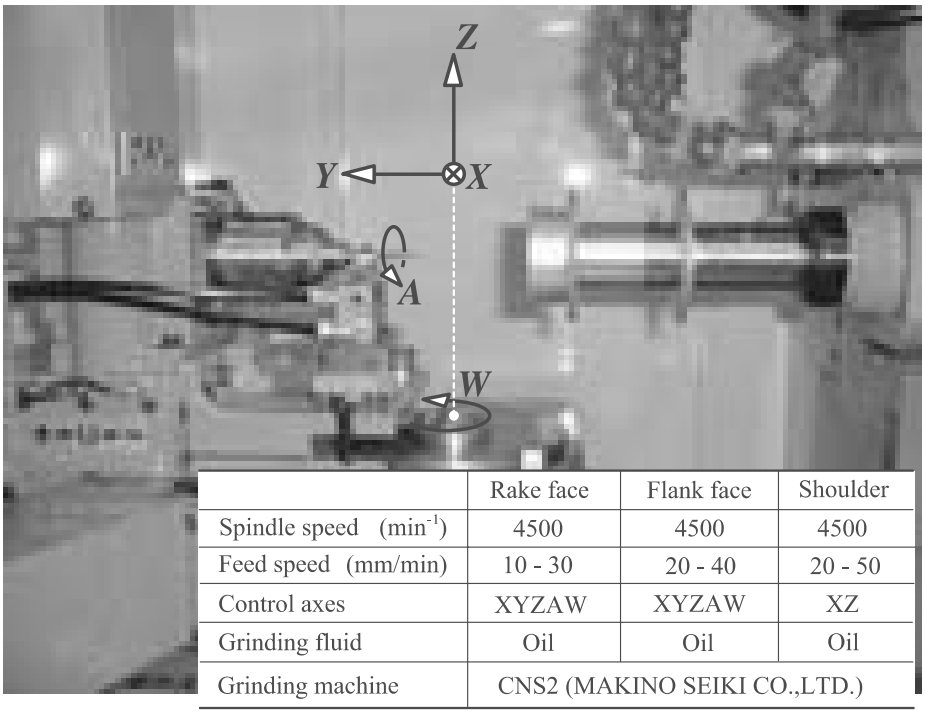

	Rake face	Flank face	Shoulder
Spindle speed (min^{-1})	4500	4500	4500
Feed speed (mm/min)	10 - 30	20 - 40	20 - 50
Control axes	XYZAW	XYZAW	XZ
Grinding fluid	Oil	Oil	Oil
Grinding machine	CNS2 (MAKINO SEIKI CO.,LTD.)		

Fig. 12. View of a tool grinding machine and grinding conditions

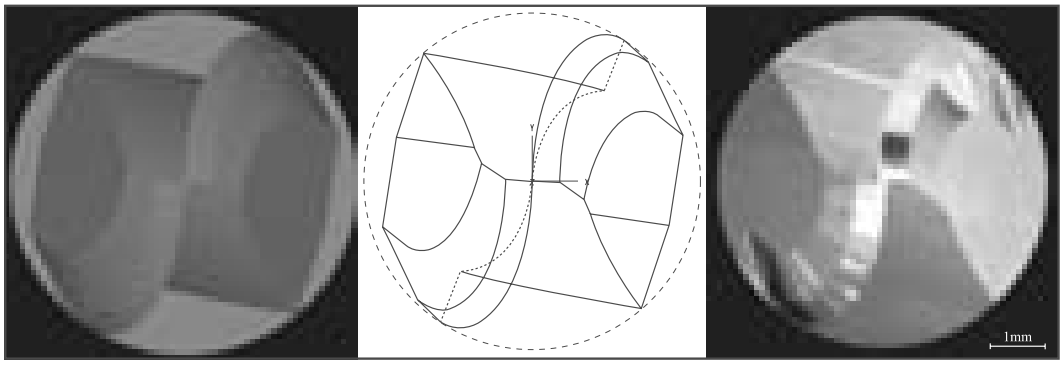

Designed ball end mill (Solid) Designed ball end mill (Wire) Fabricated ball end mill

Fig. 13. Comparison between designed and fabricated ball end mill

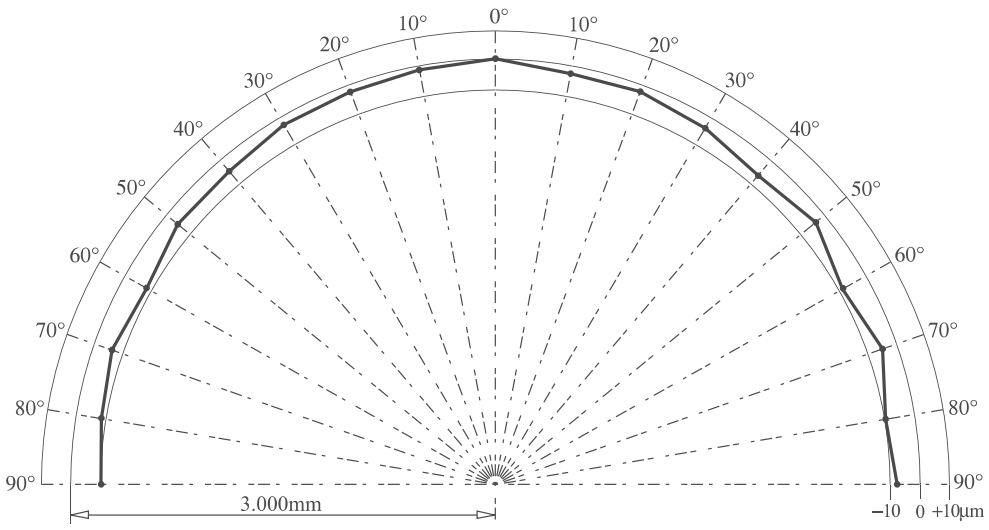

Fig. 14. Radius accuracy measurement of fabricated ball end mill

3 Fundamental investigations of cutting characteristics with different ball end mills

3.1 General information for tool shape models of ball end mills

In this section, several new types of ball end mills with different helix angle and rake angle are proposed and fabricated by the developed 3D-CAD/CAM system above. Figure 15 shows three types of available ball end mill models. From top to bottom, it is laid out with three shape models imaged, and displayed on a 3D-CAD, the top views of each model show the helix angles as well as the side views for the rake angles. For the sake of convenience, the study identifies and names each ball end mill model by its helix angle and rake angle. As shown in the top and side views of Fig. 15, the letter "P" (positive) is given to the helix angles and rake angles to express a positive degree, while the letter "N" (negative) is used to represent a negative degree. Additionally, symbol "/" is placed between the helix angle and rake angle to represent a ball end mill. For example, a ball end mill with a helix angle $\lambda(+30°)$ and a rake angle $\gamma(-10°)$ can be named P30/N10. Utilizing these notations, the three basic ball end mill models are called N/N, P/N and P/P, respectively.

3.2 Creation of ball end mills with different tool shapes

Table 1 shows 14 different ball end mills designed and fabricated, with four helix angles ($45°, 30°, 10°, -10°$) combined with five rake angles ($30°, 20°, 10°, 0°, -10°$). Fine-grained cemented carbide was applied to the tool material and the tool diameter was 6 mm.

The commercially available tool grinding machine shown in Fig. 12, with three translational axes (X,Y,Z) and two rotational axes (A,W), was used for ball end mill manufacturing. Two types of wheel, a straight wheel (SDC400N150B, for rake face and shoulder grinding) and a cup wheel (SDC600N150B, for flank face grinding), were adopted. Fourteen types of ball end mills were fabricated successfully by use of the developed CAM system.

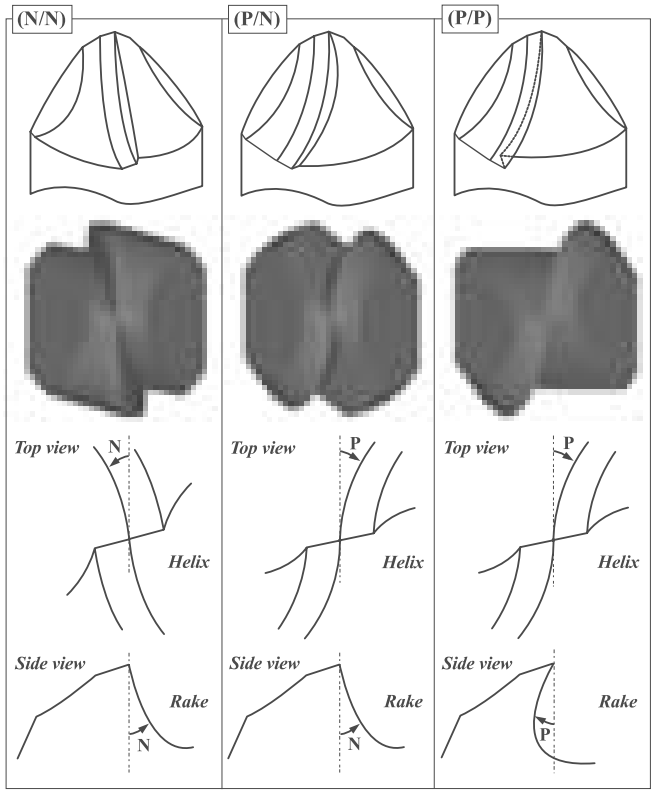

Fig. 15. Three basic ball end mill models for investigation

Table 1. Fabricated ball end mills for cutting experiments

Rake (γ) / Helix (λ)	30	20	10	0	−10
45	P45/P30	P45/P20	P45/P10	P45/P0	P45/N10
30	P30/P30	P30/P20	P30/P10	P30/P0	P30/N10
10	—	—	P10/P10	P10/P0	P10/N10
−10	—	—	—	—	N10/N10

3.3 High-speed milling experiments and evaluations

High-speed milling experiments were done using the 14 types of fabricated ball end mills on a commercially available machine tool. The machine tool and cutting conditions are shown in Fig. 16. In order to investigate the tool cutting performance, the maximum flank wear width (*VBmax*) and the workpiece surface roughness (*Ry*) were measured after each 32m cutting. Each type of ball end mill was tested three times and the averaged results were used in the evaluation. This study defines tool life as the total cutting length when the maximum flank wear width (*VBmax*) reaches 0.2 mm. Through the cutting conditions, the theoretical surface roughness was about 3.75 μm. To set up common criteria, commercially available ball end mills with the same tool material and tool radius were adopted to compare with the originally fabricated tools.

Figure 17 shows all the total experiment results with originally fabricated tools classified by helix angles, together with commercially available tools. The horizontal axis shows the cutting length, and the left hand and right hand vertical axes show flank wear (*VBmax*) and surface roughness (*Ry*), respectively. The study evaluates these cutting results from the following three viewpoints.

1. Cutting edge shape deformation:
   It is noted that the machining accuracy can be greatly influenced by the cutting edge shapes that have been damaged by such means as chipping or breakage. For the same cutting length, a tool with less cutting edge shape deformation is desirable.
2. Tool wear:
   Under the same cutting conditions and for the same cutting length, less flank wear means longer tool life. The study distinguishes less tool wear with higher cutting performance.
3. Workpiece surface integrity:
   Surface roughness is evaluated on the formed workpiece surface. The study takes into consideration both the measured roughness value and the differences of roughness value during machining.

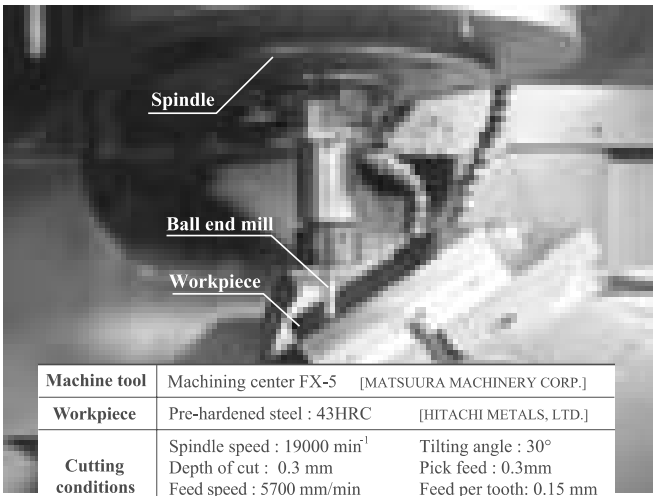

Machine tool	Machining center FX-5 [MATSUURA MACHINERY CORP.]	
Workpiece	Pre-hardened steel : 43HRC [HITACHI METALS, LTD.]	
Cutting conditions	Spindle speed : 19000 min^{-1} Depth of cut : 0.3 mm Feed speed : 5700 mm/min Cutting speed : 296 m/min	Tilting angle : 30° Pick feed : 0.3mm Feed per tooth: 0.15 mm Dry and down cutting

Fig. 16. View of a machining center and cutting conditions

3.4 Evaluation of cutting edge shape deformation

Figure 18 shows the worn cutting edge shapes with different ball end mills when each maximum flank wear width (*VBmax*) has reached 0.2 mm. The left hand side of each picture shows the top of cutting edge, and the right hand side shows the end. According to these results, it is very clear that the peripheral cutting edges represent bigger deformations when the rake angle γ varies from negative to positive (e.g., $\lambda = 45°$). It can be said that the cutting edge strength decreases as the wedge angle becomes smaller with the rake angle γ varying from negative to positive. Thus, the cutting edge strength dose needs to be taken into consideration under high-speed cutting conditions in order to prevent edge shape deformation. With a dual goal of maintaining cutting edge shape accuracy and machining accuracy, using a ball end mill with a large wedge angle, which always has a negative rake angle, is desirable for high-speed milling.

3.5 Evaluation of tool wear

Figure 19 shows the relationship between the tool life and rake angle as classified by different helix angles. Although ball end mills with negative rake angles show lesser cutting edge shape deformations, this does not necessarily mean that they have longer tool lives in each helix series (e.g., P30/N10 and P45/N10). In this case, it can be predicted that the increased cutting resistance, caused by a large wedge angle of cutting edge, reduced tool life.

In addition, Fig. 19 shows the influences on tool lives that have different helix angles. One can see that ball end mills with bigger positive helix angles (e.g., $\lambda = 45°$) have shorter tool lives and there is less of a difference of tool lives with rake angles. It is predicted that as the real cutting edge length for cutting becomes longer along with the helix angle varying to a bigger positive value, the cutting heat may be a serious factor influencing tool life (e.g., $\lambda = 45°$).

Figure 19 indicates that tool lives are influenced by both helix angles and rake angles, which complicate the cutting mechanism and cutting aspect, such as cutting resistance, cutting heat, etc., during machining. Addressing only flank wear, N10/N10 shows the longest tool life. However, the integrity of the formed workpiece surface must be taken into consideration to determine a perfect tool.

3.6 Evaluation of formed workpiece surface integrity

From Fig. 19, four originally fabricated ball end mills with the longest tool lives in each helix series together with their surface roughness results, and the results of a commercially available tool are shown in Fig. 20. The tool life curve and surface

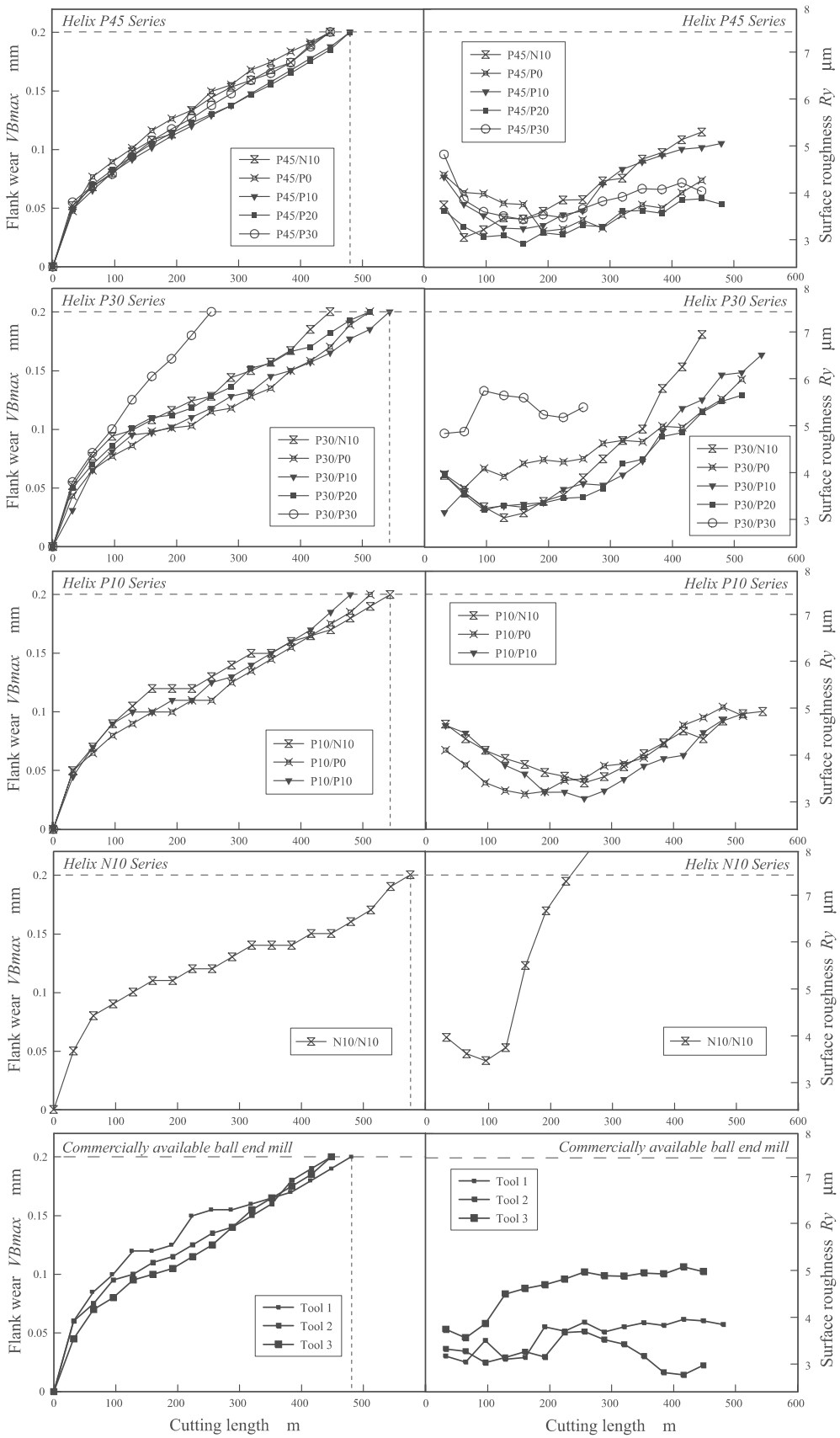

Fig. 17. Flank wear and surface roughness of different ball end mills

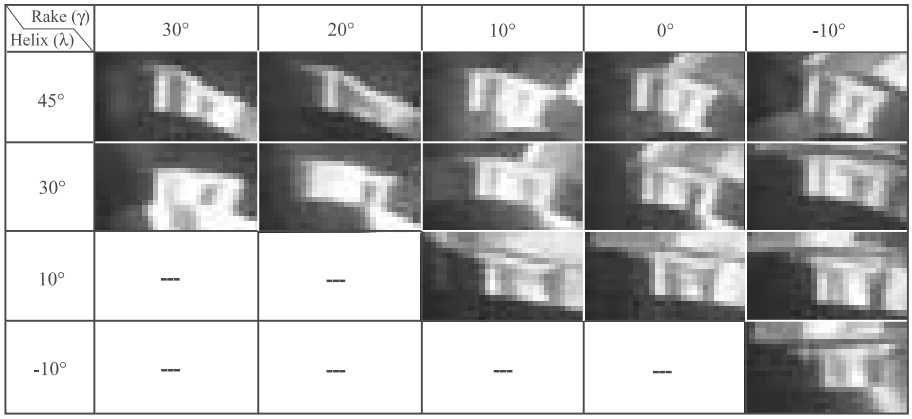

Fig. 18. Worn cutting edge shapes of different ball end mills

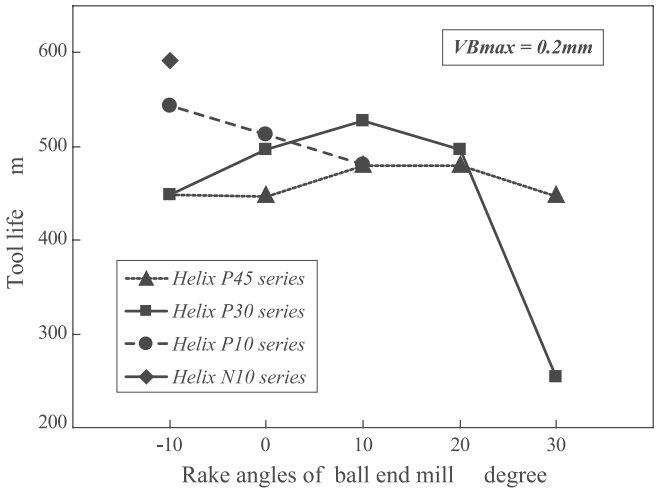

Fig. 19. Tool life curves of different ball end mills

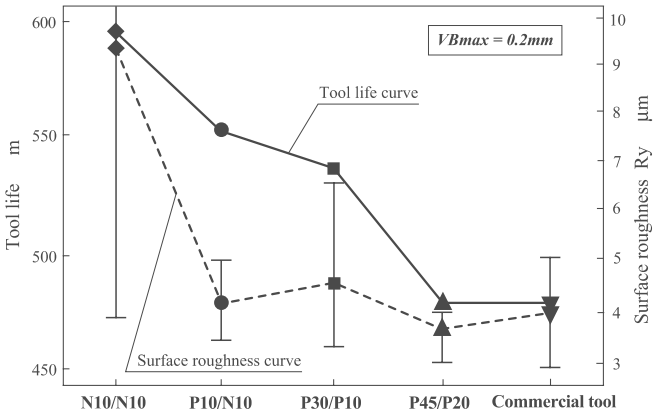

Fig. 20. Tool lives and surface roughness with different ball end mills

roughness curve are identified with a solid line and interrupted line, respectively. Vertical bars are used to represent the surface roughness differences during machining. The tool life can be seen as becoming longer when both the helix angles and rake angles turn negative (from the right hand side to the left hand side). However, the surface roughness with N10/N10 deteriorates

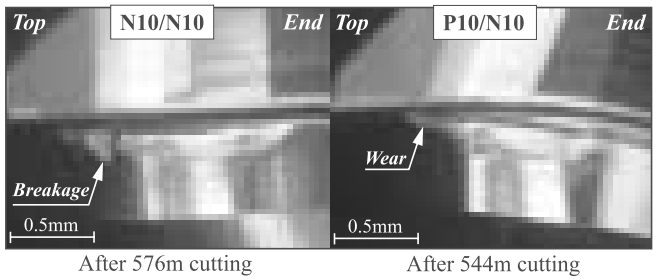

Fig. 21. Different patterns of flank wear with different tool shapes

immediately. It can be considered that the parameter of the helix angle influences the surface roughness in comparison with P10/N10, which shows stable surface roughness.

Figure 21 shows the cutting edge shapes of N10/N10 and P10/N10 after cutting. It is clear that the wear patterns are quite different close to the top portion of each cutting edge. It can be predicted that the breakage, occurring at the top edge portion of N10/N10, gravely damaged the surface integrity. Breakage was not found in other types of ball end mills with positive helix angles. Accordingly, to achieve stable surface integrity, it seems that it is necessary to set the helix angle to a positive degree. Otherwise, there is a risk of cutting edge breakage, which may be regarded as occurring due to bad chip removal direction.

By means of investigating the tool shape deformation, tool life and surface integrity, together with the influences on cutting resistance, cutting heat and chip removal direction, one can see that P10/N10 shows the best cutting performance among all fabricated ball end mills and commercially available ones in high-speed milling.

4 New proposals of ball end cutting edge shapes with micro-land treatment

4.1 Proposals of ball end mill with p-land and n-land

In Sect. 3, the understanding that (1) a large wedge angle to maintain cutting edge shape accuracy, and (2) a positive helix angle to easily remove chips are indispensable. One solution

to set a negative rake angle to achieve a large wedge angle was explored. However, it is also indicated that a negative rake angle causes high cutting resistance which may decrease the tool life and damage workpiece surface integrity. In order to solve the conflicting problem, the study proposed n-land and p-land shapes to ball end cutting edges, respectively. Two ball end mills, P30/P10 and P30/N10, were set as basic tool models. The purposes are explained below:

1. Originally fabricated helix P30 series ball end cutting edge shapes are close to commercially available ones. It is easy to apply the land treatment effects to commercial ball end mill developments.
2. Focusing on the advantages of small cutting edge shape deformation with an N10 rake angle, and small cutting resistance with a P10 rake angle, the study proposes a ball end mill with both of the advantages by means of micro-land treatment to improve tool life and achieve stable surface integrity.

Figure 22 shows the image of a proposed ball end mill with n-land. The study defines a micro-land with a negative angle ($\gamma' = -10°$) as n-land, between the rake face and the cutting edge curve, to improve the strength of the cutting edge. And the rake face part is set with a positive rake angle ($\gamma = 10°$) to reduce cutting resistance next to the n-land. The n-land ball end mill is named P30/P10/n10. At the bottom of Fig. 22, two illustrations show the edge shape differences of ball end mills with negative rake angle and n-land.

There are two important reminders that must be dealt with when using the n-land shape design:

1. The land treatment process is different from conventional honing process, since the n-land part is considered as one part of the cutting edge shape. That is, the cutting edge radius accuracy of a solid ball end mill will not be damaged by n-land treatment.
2. To reduce cutting resistance, the n-land width (Wn) must be designed smaller than the actual depth of cut. Additionally, the n-land has to be designed with a different width at each cutting edge position since two cutting edge curves cross at the top point O. The study defines the n-land width, starting at the edge top point ($Wn = 0$ mm) and ending at the edge end

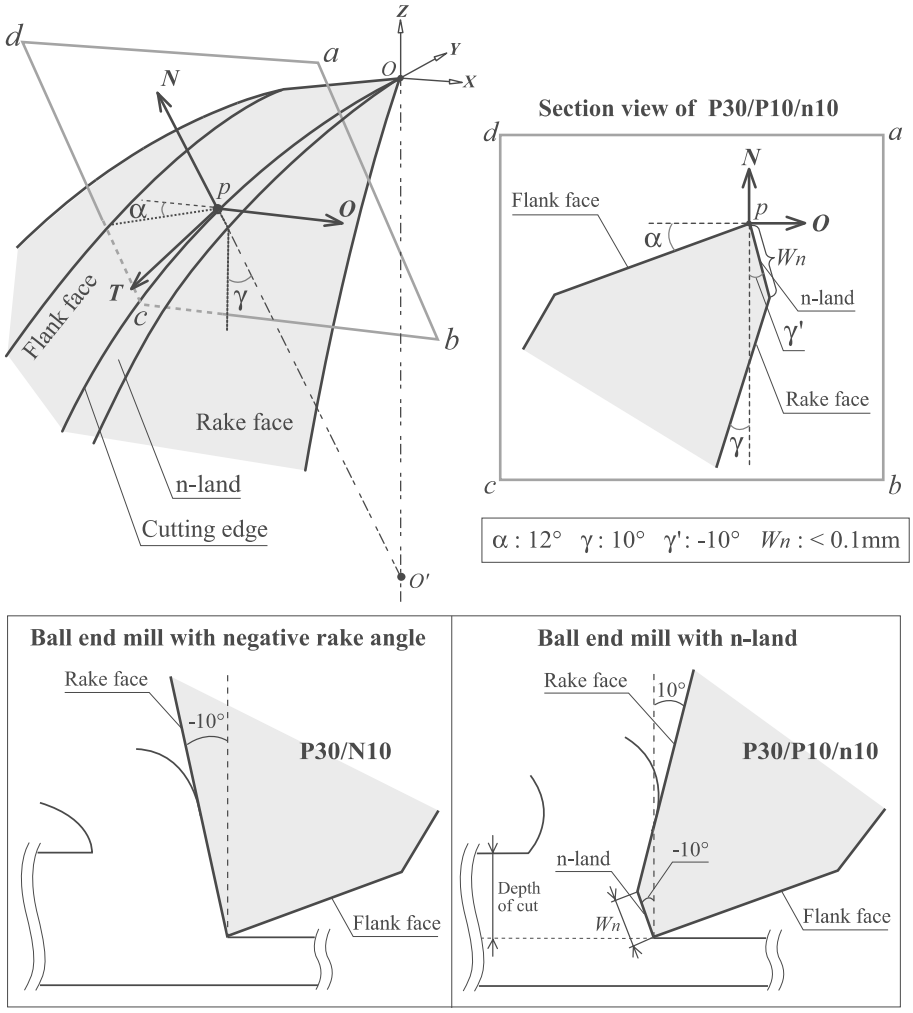

Fig. 22. Explanation of a ball end mill with n-land treatment

point (Wn = 0.1 mm), since the actual depth of cut is set to 0.3 mm.

Figure 23 shows another land shape proposal called p-land to achieve the same purpose of n-land treatment. The study defines the p-land as having a tilting angle ($\alpha' = 5°$), smaller than the clearance angle ($\alpha = 12°$) between the flank face and the cutting edge curve, to improve the strength of the cutting edge. To prevent the risk of lowering machining flexibility, the p-land width (Wp) is set with a small value. The study designed four p-land ball end mills with the widths of 0.02 mm, 0.04 mm, 0.10 mm and 0.13 mm. Each p-land width remained constant through the entire cutting edge. At the bottom of Fig. 23, two illustrations show the edge shape differences of a ball end mill with a positive rake angle and p-land. The study also made a p-land ball end mill with a positive rake angle ($\gamma = 10°$) and named it P30/P10/p5.

4.2 Creation and evaluation of ball end mills with micro-lands

Based on the micro-land proposals of n-land and p-land, new functions for creating land shapes are developed and plugged into the 3D-CAD/CAM system. Figure 24 shows the successfully fabricated n-land and p-land ball end mills using the extended CAM system. Each type of land tools (n-land: one type, p-land: four types) was fabricated and applied to high-speed milling experiments three times. Figure 25 shows the experimental results of the n-land ball end mills.

The results of P30/P10 and P30/N10 were added to Fig. 25 to compare with the n-land ball end mill. It was discovered that the tool lives particularly increased while the surface roughness curves remained comparatively stable. Figure 26 shows the cutting edge shape deformation after 416 m cutting between the n-land tool and P30/P10. Comparing it with the n-land ball end mill, P30/P10 has a larger area of deformation. It can be understood that a ball end mill with n-land effectively maintains cutting edge shape accuracy.

Figure 27 shows the experimental results of the p-land ball end mills. With Fig. 27, one can see that the experimental results were separated into two types with different p-land widths. The tools with large widths (Wp = 0.10 mm, 0.13 mm) show short tool lives and unstable surface roughness. On the other hand, the tools with small widths (Wp = 0.02 mm, 0.04 mm) show improved tool lives and stable surface roughness. Figure 28 compares the tool wear between two p-land tools (Wp = 0.04 mm,

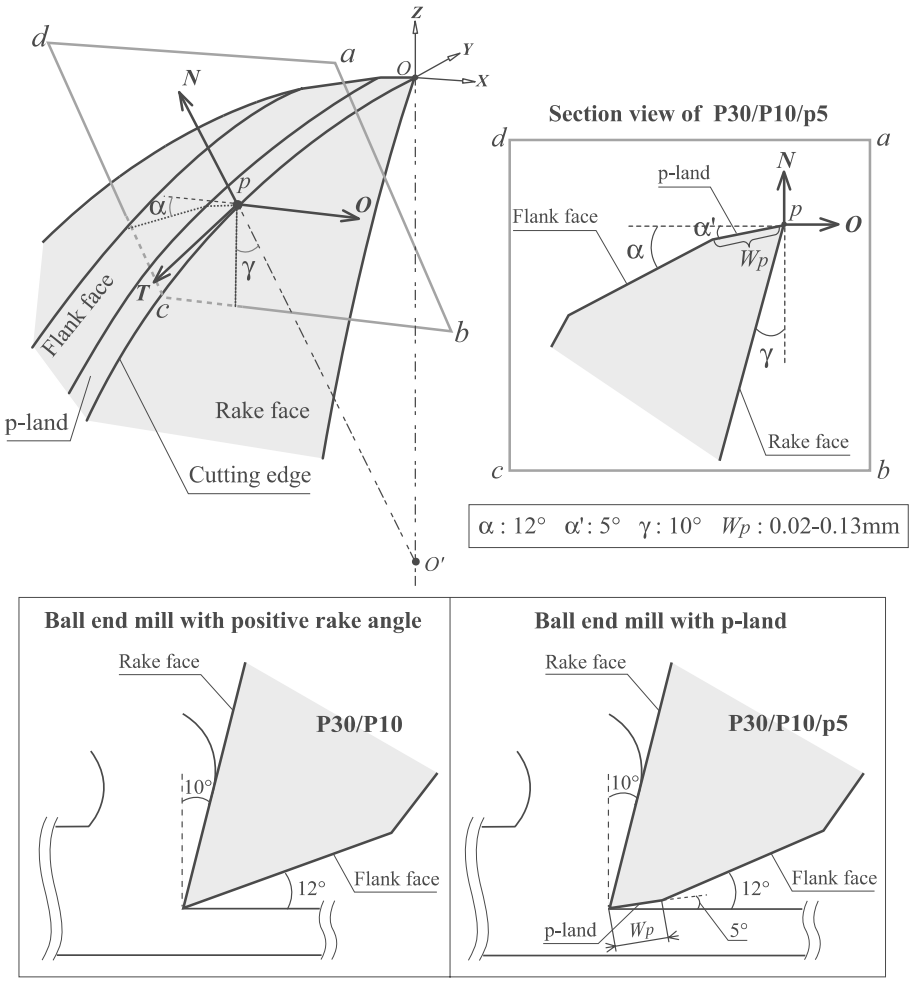

Fig. 23. Explanation of a ball end mill with p-land treatment

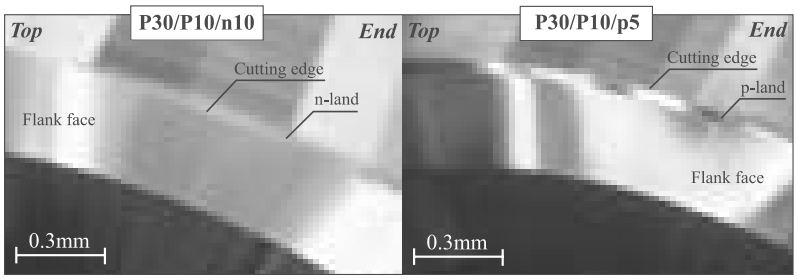

Fig. 24. Fabricated n-land and p-land ball end mills

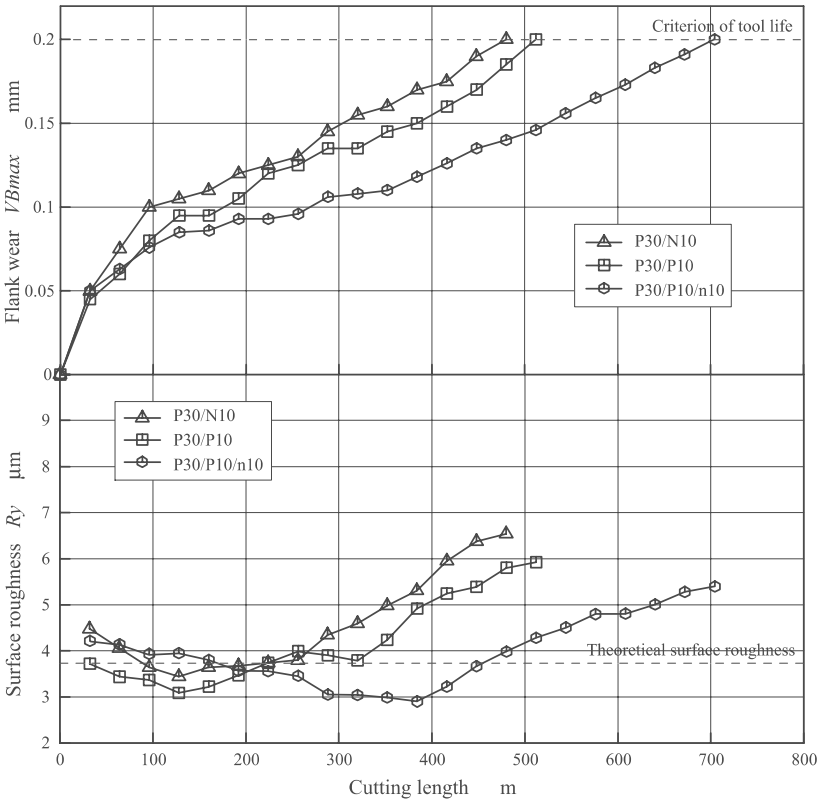

Fig. 25. Experimental results with n-land ball end mills

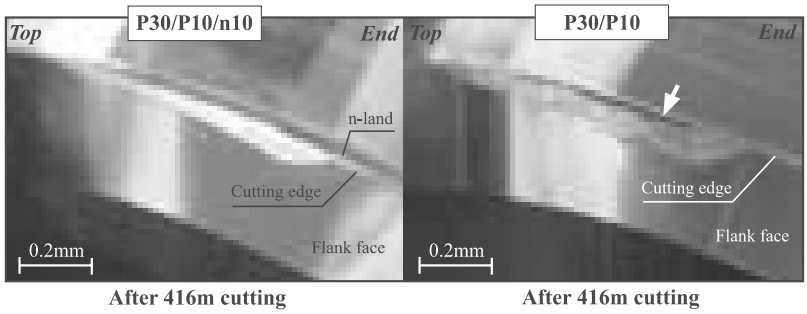

Fig. 26. Comparison of cutting edge shape deformation

0.10 mm) after 416 m cutting. One can see that the wear patterns are quite different on the top edge portions so it can be said that greater flank wear on the top edge portion causes worse surface roughness. The tool with a p-land width of 0.04 mm showed the highest cutting performance among the four p-land tools. Although a p-land tool with a small land width showed a better cutting performance than P30/P10 (Fig. 27), it does not seem that the effect on preventing cutting edge shape deformation is re-

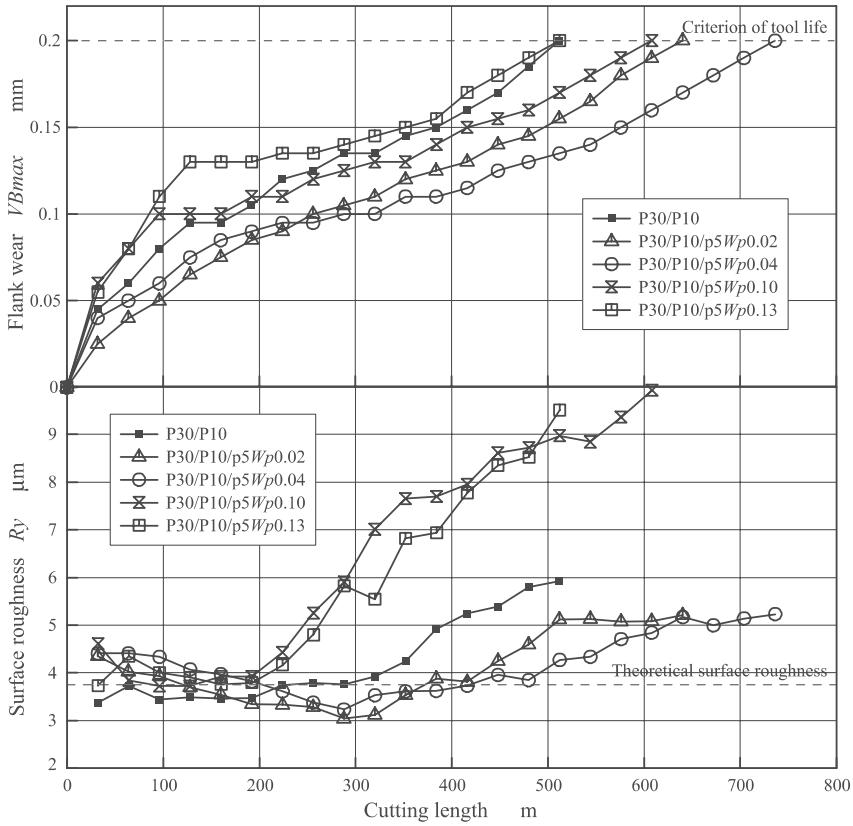

Fig. 27. Experimental results with p-land ball end mills

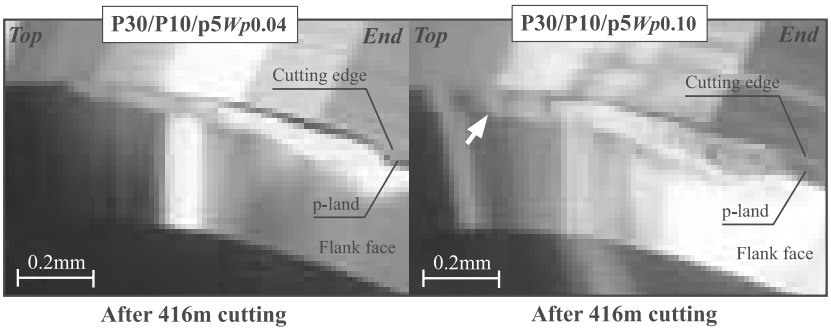

Fig. 28. Comparison of tool wear with different p-land tools

markable with a p-land. The reason being that the wedge angle cannot be enlarged enough to improve the strength of the cutting edge by means of a p-land treatment.

5 Proposal of ball end mill with n-p-land treatment

Based on the investigations of the cutting performance of ball end mills with n-land and p-land treatment, Fig. 29 shows a newly designed and fabricated ball end mill with n-p-land, which was expected to achieve a much higher cutting performance. A ball end mill with n-p-land is used to mean one that has both n-land and p-land treatments applied to its cutting edge. The shape parameters used for the n-p-land have been taken from the evaluated n-land and p-land ball end mills explained above. The bottom pictures of Fig. 29 show enlarged views of the n-p-land ball end cutting edge, which was successfully fabricated. The study names the tool P30/P10/n10/p5.

Using the same cutting conditions shown in Fig. 16, high-speed milling experiments with n-p-land ball end mills were conducted. The experiment results are shown in Fig. 30. The tool life curves and surface roughness curves show the measured data with three n-p-land ball end mills. It was found that among all the previous experiments, the n-p-land ball end mill showed the longest tool life, and smallest difference of surface roughness varying within the range of ± 1 μm to the theoretical value (3.75 μm). Not only were the surface roughness differences less, but also the tool wear differences among the three tests were also

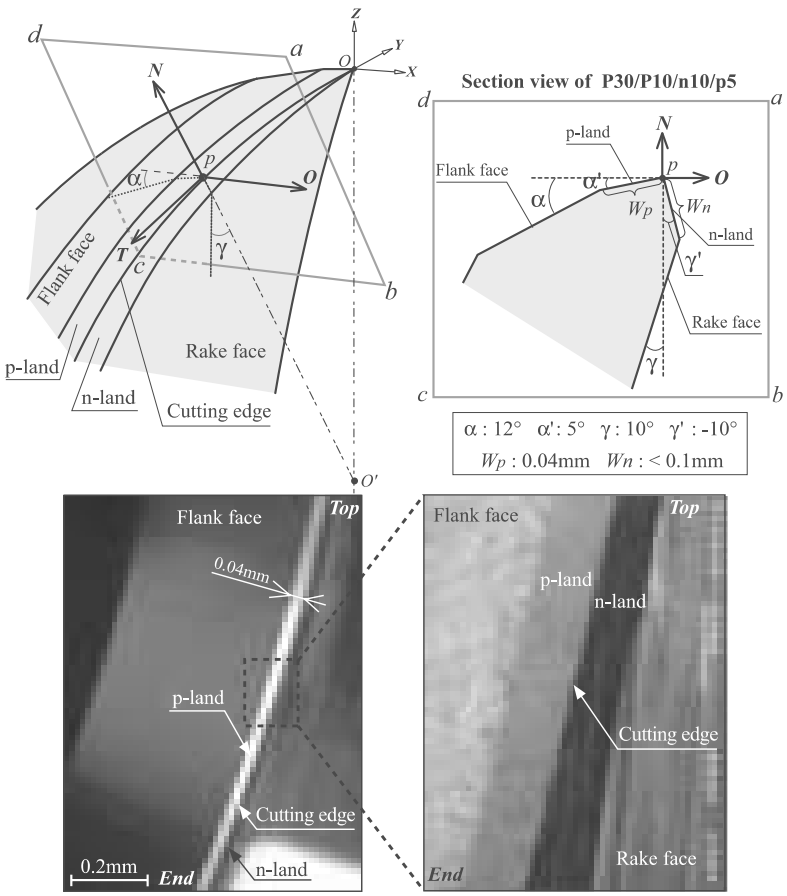

Fig. 29. Designed and fabricated n-p-land ball end mill

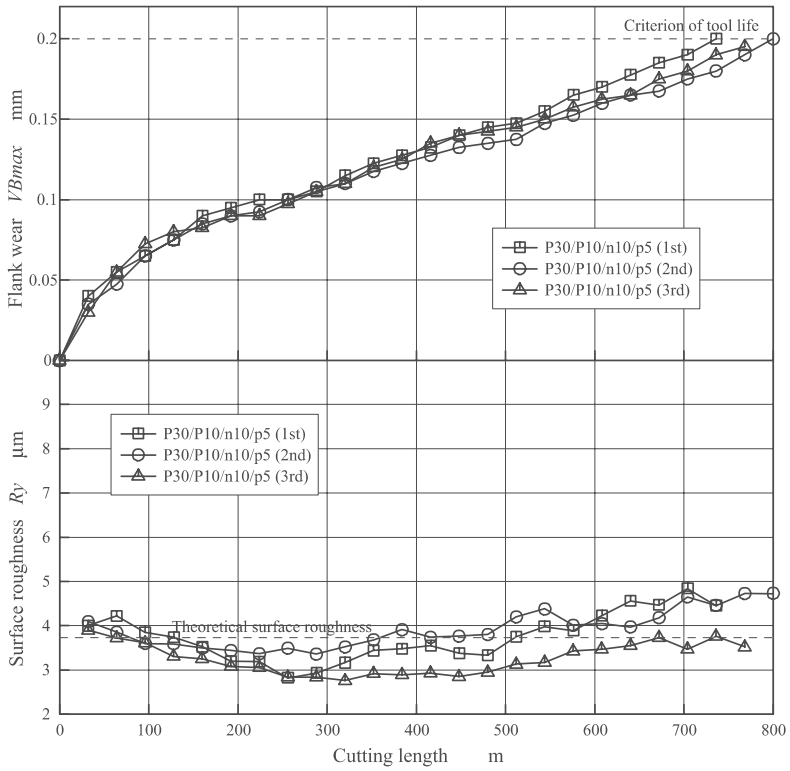

Fig. 30. Experimental results with n-p-land ball end mills

significantly small. Figure 31 shows the tool wear growth of the n-p-land tool. Tool wear grew stably and unexpected chipping was not found during the whole machining. Based on these evaluations, it can be ascertained that the proposed ball end mill with n-p-land treatment shows the highest cutting performance and is the most suitable ball end cutting edge shape for high-speed milling.

Figure 32 shows the experiment results concerning ball end mills P30/N10, P30/P10, P30/P10/n10, P30/P10/p5 and P30/P10/n10/p5. Looking at this figure beginning on the left hand side and progressing to the right, one can see that the differences of surface roughness becomes less while the tool life increases. This figure strongly shows the validity of micro-land treatment.

6 Conclusion

Focusing on the optimization of the cutting edge shape of a ball end mill, the study developed and proved a reasonable tool design, creation and evaluation system. It is the first such development for a ball end mill created using a 3D-CAD/CAM system. The study is summarized as follows:

1. A ball end mill design and creation 3D-CAD/CAM system was successfully developed and applied for ball end mill fabrication. This indicated the applicability of the developed system.
2. Several new types of ball end mills with different rake angles and helix angles were fabricated successfully with the

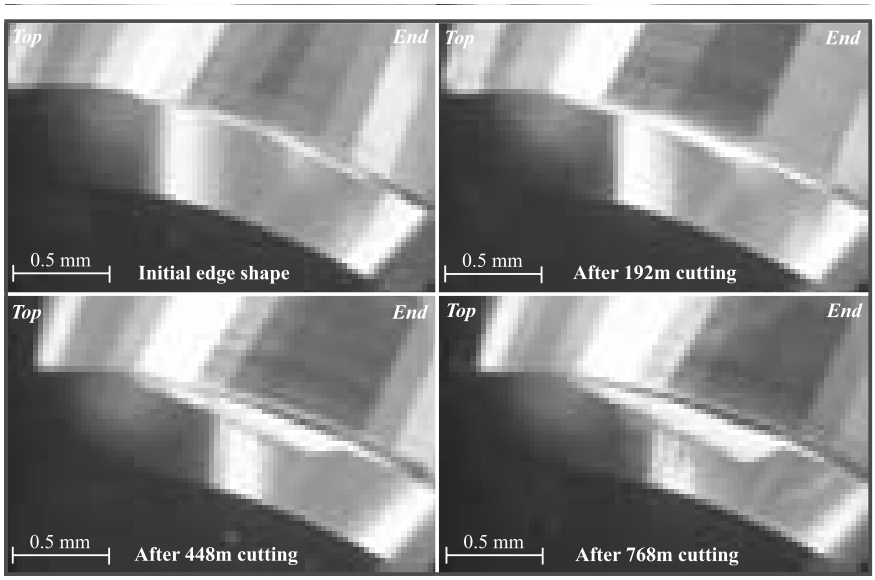

Fig. 31. Tool wear growth of n-p-land ball end mill

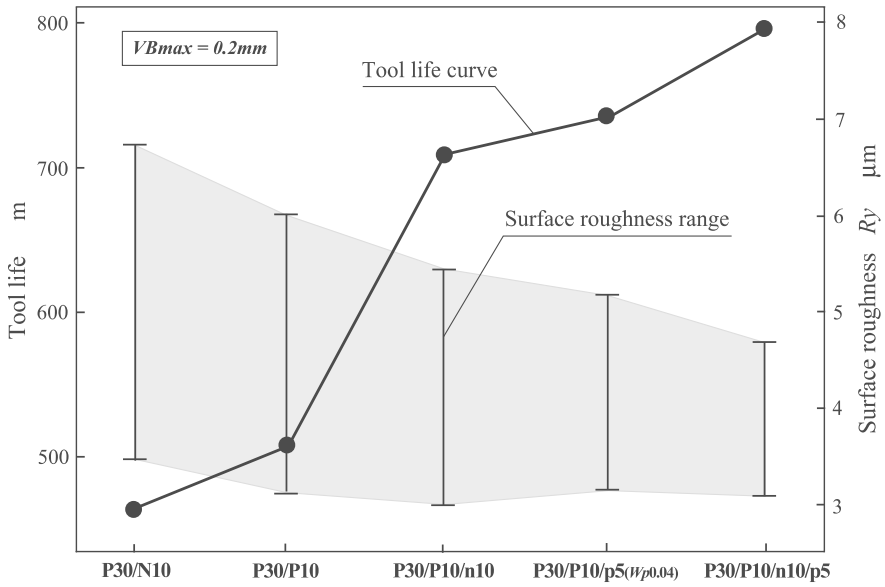

Fig. 32. Total evaluation of proposed ball end mills

developed system. By means of high-speed milling experiments, it was found that P10/N10 was the most suitable tool shape for high-speed milling among all of the investigated ball end mills. In addition, essential conditions of ball end cutting edge shape for high-speed milling were clarified.

3. Based on the fundamental investigations above, to solve the conflicting problem of the increased strength of cutting edge (advantage) and increased cutting resistance (disadvantage) by setting a negative rake angle to a cutting edge, the study newly proposed ball end mills with n-land and p-land. Both of these were fabricated successfully by the developed CAM system and evaluated experimentally.
4. By using the finest land shape parameters determined above, the study additionally proposed n-p-land ball end mill and fabricated it successfully. It was found that this tool displayed the highest cutting performance among all ball end mills investigated by evaluating the cutting edge shape deformation, tool life and workpiece surface integrity. Thus, a ball end mill with n-p-land should be considered as the most suitable edge shape model for high-speed milling.
5. Through the above developments and investigations, it is evident that the developed ball end mill design, creation and evaluation system shows higher flexibility and validity compared to commercially available tool manufacturing systems for new tool development.

Acknowledgement The authors would like to express their sincere appreciation to Dr. K. Morishige (University of Electro-Communications), Dr. T. Matsuoka (MATSUOKA Engineering Consultants Office Ltd.), Dr. K. Kase and Dr. K. Sunouchi (Institute of Physical and Chemical Research) for their valuable support and information.

References

1. Altan T (1993) Advanced techniques for die and mold manufacturing. Ann CIRP 42(2):707–716
2. Gaida W, Rodriguez C, Altan T, Altintas Y (1995) Preliminary experiments for adaptive finish milling of die and mold surfaces with ball-nose end mills. Trans NAMRI/SME 23:193–198
3. Heisel U, Gringel M (1997) Machine tool design requirements for high-speed machining. Ann CIRP 46(1):389–392
4. Tsutsumi M, Saito A (2003) Identification and compensation of systematic deviations particular to 5-axis machining centers. Int J Mach Tools Manuf 43:629636
5. Weck M, Schubert I (1994) New interface machine/tool: hollow shank. Ann CIRP 43(1):345–348
6. Rivin E (2000) Tooling structure: interface between cutting edge and machine tool. Ann CIRP 49(2):591–634
7. Schulz H, Moriwaki T (1992) High-speed machining. Ann CIRP 41(2):637–643
8. Schulz H, Hock S (1995) High-speed milling of die and molds – cutting conditions and technology. Ann CIRP 44(1):35–38
9. Takahashi I, Anzai M, Nakagawa T (1999) Wear characteristics of small WC ball end mill at 100 000/min milling. J JSPE 65(5):867
10. Dewes RC, Aspinwall DK (1997) A review of ultra high-speed milling of hardened steels. J Mater Process Technol 69:1–17
11. Vichers G, Quan K (1989) Ball-mills versus end-mills for curved surfaces milling. ASME J Eng Ind 111:22–26
12. Takeuchi Y, Nagasaka M, Morishige K (1996) 5-axis control machining with top and side cutting edges of ball end mill. J Adv Autom Technol 8(1):30–36
13. Choi B, Jun C (1989) Ball-end cutter interference avoidance in NC machining of sculptured surfaces. Comput Aided Des 21(6):371–378
14. Takeuchi Y, Watanabe T (1992) Generation of five-axis control collision-free tool path and post processing for NC data. Ann CIRP 41(1):539–542
15. Nagasaka M, Takeuchi Y (1996) Generalized post-processor for 5-axis control machining based on form shape function. J JSPE 62(11):1607–1611